

Multifocal ERG Recordings Under Visual Control of the Stimulated Fundus in Mice

Ralf M. Dutescu,^{1,*} Sergej Skosyrski,¹ Norbert Kociok,¹ Irina Semkova,¹ Stefan Mergler,¹ Jenny Atorf,² Antonia M. Joussem,¹ Olaf Strauß,¹ and Jan Kremers²

¹Department of Ophthalmology, Charité Universitätsmedizin Berlin, Berlin, Germany

²Department of Ophthalmology, University Hospital Erlangen, University of Erlangen-Nuremberg, Erlangen, Germany

Correspondence: Norbert Kociok, Charité Universitätsmedizin Berlin, Department of Ophthalmology, Augustenburger Platz 1, D-13353 Berlin; Norbert.Kociok@charite.de. Ralf M. Dutescu, Charité Universitätsmedizin Berlin, Department of Ophthalmology, Augustenburger Platz 1, D-13353 Berlin; dutescumichael@googlemail.com.

RMD and SS contributed equally to the work presented here and should therefore be regarded as equivalent authors.

Current affiliation: *ACTO e.V., Karlsburgerweg 9, 52170 Aachen, Germany.

Submitted: December 6, 2012

Accepted: March 13, 2013

Citation: Dutescu RM, Skosyrski S, Kociok N, et al. Multifocal ERG recordings under visual control of the stimulated fundus in mice. *Invest Ophthalmol Vis Sci*. 2013;54:2582-2589. DOI:10.1167/iovs.12-11446

PURPOSE. Therapeutic approaches to retinal disease require a continuous monitoring of functional improvement over lesion areas that sometimes cannot be shown in full-field ERG. The aim of this study was to assess the usefulness of multifocal electroretinograms (mfERGs) under visual control using scanning laser ophthalmoscopy (SLO) for evaluation of local retinopathy in mice.

METHODS. mfERGs were optimized for recordings in C57BL/6 mice by varying dark steps between each stimuli, background intensity, and the numbers of hexagons. Local retinopathy was induced by argon laser photocoagulation with different spot sizes and retinal irradiances. mfERG recordings were performed before, and 10 days and 4 weeks after laser treatment. In each recording, the central hexagon was positioned on the optic nerve head visualized by SLO images. The amplitudes of the P1 response components were analyzed as a function of retinal location.

RESULTS. The mfERG amplitudes depended on stimulus condition. The P1 amplitudes increased with increasing number of dark frames in the m-sequence and with decreasing number of hexagons. A stimulus with 19 hexagons and four dark frames was chosen because substantial response amplitudes could be achieved while preserving sufficient spatial resolution. In the untreated eyes, the response to the central hexagon, stimulating the optic nerve head, was smaller than those to the surrounding hexagons. The responses to hexagons stimulating photocoagulated areas were reduced compared with the responses of surrounding areas. The amplitude reduction was more pronounced when the coagulated areas were larger and when higher energies were used.

CONCLUSIONS. Areas with decreased sensitivities to light stimulation (either the optic nerve head or damaged retinal areas) can be detected and correlated with the retinal images and in the mfERG responses. We demonstrate that the mfERG technique is able to reproducibly detect the functional consequences of a local treatment.

Keywords: multifocal ERG, scanning laser ophthalmoscopy (SLO), retinal imaging, laser photocoagulation

The electroretinogram (ERG) is a useful tool for assessing mainly outer retinal function.¹ Full-field ERGs reflect mass potential changes that originate in activity of the complete retina. However, spatial variations in the ERG responses are not assessed. In 1992, Sutter and Tran² first introduced the multifocal ERG (mfERG) technique, which provides a functional topographic map of the central retina. In retinal research and for pharmacological studies, rodents are routinely used as a disease model. Furthermore, full-field ERG is widely used to monitor functional changes due to either degenerative processes or therapeutic success. However, degenerative processes can be local and therefore only weakly contribute to changes in the full-field ERG. Thus, to analyze the spatial distribution of effects from the retinal disorders and/or of treatments in these models, the mfERG technique would be extremely useful. It permits the functional analysis of local structural changes in the living animal. However, before mfERG recordings can be implemented routinely, several technical problems have to be solved. Ball and Petry³ first recorded

mfERGs in the rat. They were able to show that mfERGs were recordable but there were major limitations with this method. First, in rodents, an ERG is mostly rod driven, whereas the mfERG in humans is highly cone dependent. Therefore, stimulus frequency should be reduced to allow the rod system to respond. Second, the relatively small size of the retina of the rat model enhanced the occurrence of stray light artifacts. Third, in animals without a fovea, a control of the position of the stimulus on the retina is absent.^{4,5} Therefore, a direct visualization of the fundus during mfERG recordings is mandatory in rodent research. In early attempts, a fundus image was taken during or after recording an mfERG.^{4,6} However, even if a fundus image is obtained, it is not clear whether the image and the mfERG stimulus are well-aligned. Accordingly, retinal landmarks are necessary in order to correlate both the image and the recording. A natural landmark is the optic nerve head (ONH); however, more landmarks are necessary to obtain a better correlation.

The aim of this study was to ascertain the feasibility of mfERG recordings in mice using defined retinal landmarks from simultaneously obtained retinal images. For future therapeutic approaches, it is important to show that a reproducible mfERG technique is able to detect functional consequences of local therapy. As a model of focal retinopathy, various local retinal damages were induced in mice by argon laser photocoagulation. The effects of the local damage on the mfERG responses were investigated. The retinæ were visualized by scanning laser ophthalmoscopy (SLO). The mfERG stimulus was projected onto the retina using a part of the optical path of the SLO. Specifically, the reproducibility of the mfERG recordings was studied. Finally, we investigated the effects of the laser spot size and energy on the mfERG amplitudes.

MATERIALS AND METHODS

Animals

The experiments were approved by the local animal ethics committee and the local authorities of Berlin and adhered to the ARVO guidelines for animal research. The experiments were carried out on 5-month-old C57BL/6 mice (Janvier, St. Berthevin, France) with a body weight between 27 and 30 g. The mice were dark adapted the night before the recordings were performed. The animals were anesthetized by a subcutaneous injection of xylazine (15 mg/kg) and ketamine (110 mg/kg). The animals were positioned on a warming table to maintain the body temperature. Of each animal, only the right eye was examined. Before recordings started, the eyes were dilated using 0.5% tropicamide (Mydriaticum stulln; Stulln GmbH, Stulln, Germany) and 1% atropine (Atropin POS 1%; Ursapharm GmbH, Saarbruecken, Germany). After mfERG recordings, dexpanthenol (Corneregel; Dr Mann GmbH, Berlin, Germany) was applied for corneal recovery. The experiments were always performed at the same time of day (between 12 AM and 5 PM).

Recording Technique

The mice were positioned 1 to 2 mm in front of the SLO device with a built-in white light source for stimulus projection (Roland Consult, Brandenburg, Germany). A DTL recording electrode was placed at the corneal limbus. Subcutaneous silver needle electrodes served as reference and ground electrodes. The SLO facility was built for use in human subjects. For application in mice, an optical correction (a double aspheric 60-dpt glass lens) was positioned in front of the exit lens of the SLO device (Volk Optical, Inc., Mentor, OH). For further magnification, a 90-dpt contact lens was used. Viscous methocel 2% gel (OmniVision GmbH, Puchheim, Germany) was applied underneath the contact lens. The methocel underneath the outer edge of the contact lens was slowly dried in order to immobilize the contact lens.

The responses were amplified (100,000 \times) and band-pass filtered (10–100 Hz). The signals were digitalized and acquired with 1024-Hz sampling frequency. The software used to generate the stimulus and to record the ERG potentials (Retimap; Roland Consult) was also used for the simultaneous acquisition of retinal images by SLO. The compact SLO plus stimulator device could be moved and rotated to optimize the image and to select the recording area. The stimulus was adjusted so that hexagons were maximally covering the ONH and coagulated areas. The ONH was covered by the central hexagon. Although the pupil of the eye often did not completely match the entrance pupil of

the stimulator, thereby stopping light and restricting the retinal image, the stimulated retinal area was not affected by this. The same stimulus configuration was used in measurement repetitions at different sessions (see below). Figure 1B shows an example of a fundus image and a sketch of the projection of a seven-hexagon stimulus. The mfERG responses to the stimuli in the respective hexagons are displayed.

Stimulus

An array of equally sized hexagons was projected on the retina (see Fig. 1B). The stimuli were generated by a projector with a refresh rate of 60 Hz. In the m-sequence, the luminance of the hexagons was either 150 cd/m² (corresponding to 2.5 cd s/m² in a single frame) or less than 1 cd/m². Please note that cd/m² is a photometric term and that the spectral output is weighted by the human luminosity function (V_{λ}), which is not relevant for the mouse. To calculate the retinal illuminance, this should be considered, as well as the fact that the eyes and the pupils of the mouse are substantially smaller than those of humans. However, the mean luminance is photopic also for the mouse. Furthermore, the relative retinal illuminance is the same for mice and humans. The m-exponent was 9, resulting in 511 m-sequences for each cycle. Eight cycles were averaged for a final result. Prior to the main experiment, the number of dark frames was varied. In addition, the background intensity (surrounding the stimulus) and the number of hexagons was varied (7, 19, and 37 hexagons). The optimal stimulus conditions were then used for the main experiment. Based on the results of these pilot studies (see Results section), the main experiments were performed with four dark frames between each m-presentation and with 19 hexagons.

Directly after placing the animals in front of the imaging system, the mfERG recordings were variable. This variability was considerably reduced by stimulating with multiple hexagons or a single hexagon (covering the same retinal area as with the multihexagon stimuli) for 10 minutes. These first recordings were disregarded in further analysis.

Laser Coagulation

To study the correspondence between mfERG data and fundus image in the main experiment local areas with light damage were experimentally induced by photocoagulation. The coagulation parameters were altered. Laser burns were induced by frequency-doubled Nd laser photocoagulation (532 nm, Valon STA, Valon Multispot Laser; Vantaa, Finland). Three laser parameters (duration [in ms], power [in mW], and spot size [in μ m]) could be chosen. The total energy (J/cm²) of each laser spot was calculated from the three settings. For each treatment, the corneal surface was covered by a cover slip moistened by methocel 2% to provide a sufficient fundus image.

The mice were treated according to one of the following regimens:

Scheme (group) 1: Three laser coagulations were applied as a triangle around the ONH of the right eyes ($n = 3$). Each laser spot had a size of 100 μ m, duration of 20 ms, an intensity of 120 mW, and a total energy of 30.6 J/cm².

Scheme 2: Laser spots of 300- μ m size (20-ms duration) were applied left and right from the ONH in right eyes ($n = 5$). The left spots (group 2) had intensities of 360 mW and a thus a total energy of 10.1 J/cm². The right spots (group 3) were produced with 1060 mW power and had a total energy of 30 J/cm².

mfERGs were recorded before laser treatment, 10 days after treatment, and 4 weeks after treatment.

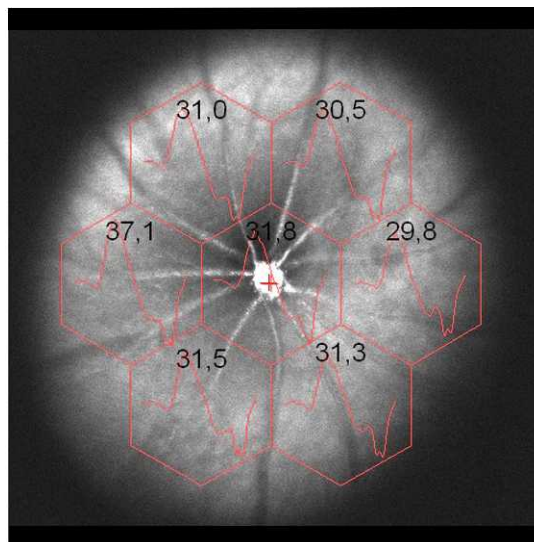
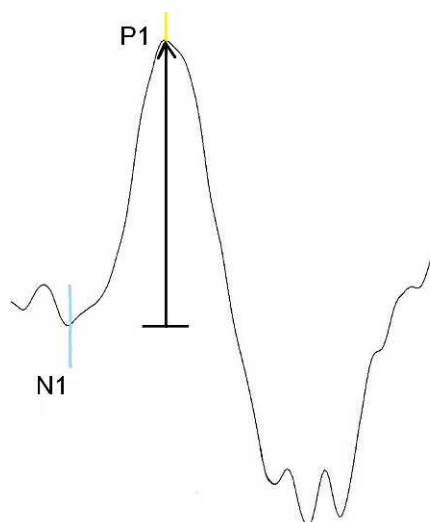


FIGURE 1. Combination of a multifocal ERG response and an SLO image of a mouse retina. (A) Example of a summed ERG response. An initial negativity (N1) is followed by a positive peak (P1). The measured amplitudes are defined by the absolute potential difference between N1 and P1 (given by the *arrow*). (B) mfERG recording with seven equally sized hexagons (*red curves*) combined with a simultaneously captured retinal SLO image. The mfERG stimulus is centered on the ONH. The mfERG amplitudes are given nV.

RESULTS

The Effect of the Number of Dark Frames and Surround Luminance

Stimuli with 12 dark frames between the m-presentations yielded larger mfERG response amplitudes than when four dark frames were used (Fig. 2). However, a measurement with 12 dark steps lasted approximately 24 minutes. During this time, it was very difficult to keep the retinal image stable because small movements (either of the stimulator or the eye) led to stimulus displacement during recordings. These movements were not observable when using four dark frames. A measurement with four dark frames lasted approximately 6

minutes. Therefore, four dark frames were used in the subsequent measurements.

In the aforementioned measurements, the area of the screen surrounding the stimulus was dark (less than 1 cd/m^2). We studied the effects of introducing a surround with different luminances (30 cd/m^2 , 150 cd/m^2). Figure 2 displays the summed response in the same animal with these surround luminances. The stimulus was an m-sequence with four darks steps between each m-presentation. Introducing a surround luminance resulted in an amplitude reduction compared to measurements without a surround.

The Effect of the Number of Hexagons

Response amplitudes of recordings with 7, 19, and 37 hexagons in two eyes are shown in Figure 3. Recordings were performed in seven eyes for each number of hexagons. Note that the amplitude of the central response displays a dip in both recordings with 19 hexagons (Fig. 3B) and in one recording with 37 hexagons (Fig. 3C). These central depressions correspond to the ONH in the SLO images. All seven eyes recorded with 19 hexagons showed a central depression. In contrast, only in a minority of the recordings with 7 hexagons (one out of seven measurements, 14%) and 37 hexagons (three out of seven measurements, 43%) was a central depression evident (Figs. 3A, 3C). In addition, recordings with 37 hexagon stimuli displayed highly variable response amplitudes (Fig. 3C). In seven tested individuals, the SEM of mfERG amplitudes increased with decreasing hexagon size (7: 1.57 μV ; 19: 1.85 μV ; 37: 2.4 μV). Based on these results, we chose stimuli with 19 hexagons to study the spatial distribution of mfERGs using local photoocoagulations.

The Effect of Retinal Location: ONH

The main aim of this study was to verify a correlation between structural retinal landmarks observed with the SLO, like the ONH, and spatial ERG distribution in retinae of the mice. As mentioned above, with a 19-hexagon array and the central hexagon positioned on the ONH, a reduced response to this central hexagon could be observed (see Fig. 3B). We further

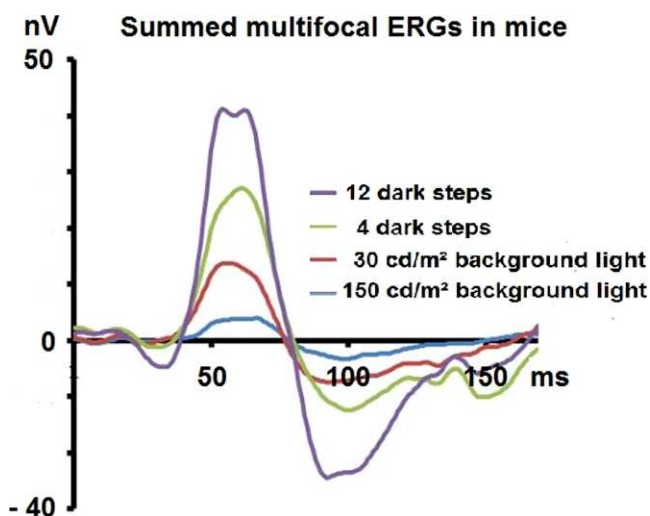


FIGURE 2. Summed multifocal ERG recordings with 19 hexagons from a single untreated mouse retina. The m-sequences with 4 and 12 dark steps without surround intensities were tested. In addition, m-sequences with four darks steps with surround intensities of either 30 or 150 cd/m^2 were tested. Comparable results have been observed in two other individuals.

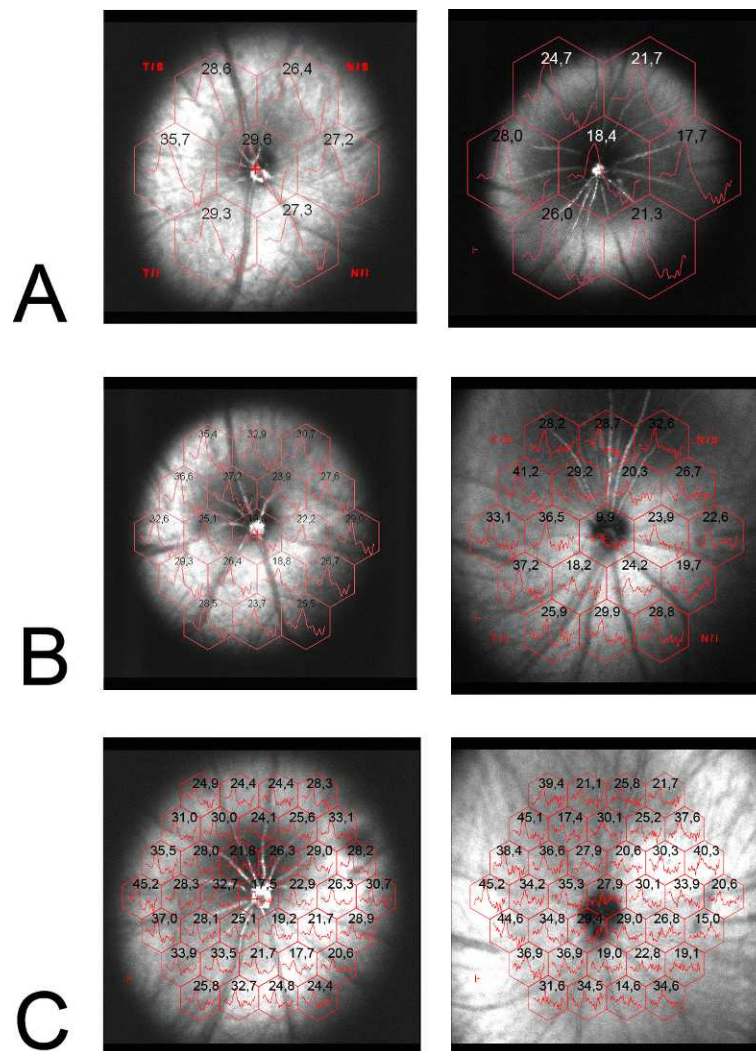


FIGURE 3. Representative examples of multifocal ERG responses in two retinæ of normal mice. Mice were stimulated with 7 (A), 19 (B), and 37 (C) hexagons, respectively. At 19 hexagons for stimulation, the lowest amplitudes were detected in the central hexagon representing the ONH area. Response amplitudes of recordings using 37 hexagons for stimulation show a central reduction for one eye (*left plot*) but not in a second eye (*right plot*). Instead, in this eye, the amplitudes vary considerably. The variable pattern was commonly found with 37 hexagon stimuli.

analyzed this effect by recording mfERGs in seven untreated mice by comparing the amplitude of the central hexagon with the mean amplitudes of the responses to the outer 18 hexagons in each individual. In Figure 4, the ERG response amplitudes to the stimulus for the central hexagon (ONH) and for the surrounding retinal areas (total retina) are given for each individual mouse. The central responses are significantly lower compared with outer retinal areas. For individuals 2 and 3, amplitude values failed the test of a normal distribution and therefore one-sample *t*-test could not be used.

The Effect of Retinal Location: Local Coagulation

Local retinal laser burns were applied to induce focal retinopathy in order to correlate structural defects with local changes in the mfERG responses. This can be detected in the SLO image. Second, we studied whether the dose and/or size of the laser photocoagulation influences the functional changes as measured with mfERG (see Figs. 5, 6).

In a first scheme, three laser spots of 100- μ m diameter and energies of 30.6 J/cm² were applied at the corners of an imaginary triangle surrounding the ONH. In Figure 5, the results obtained in two mice are displayed. SLO images with

superimposed mfERG recordings are shown before, and 10 days and 4 weeks after focal laser treatment. These laser spots appeared as darker regions (encircled) in the SLO images. Here, no laser effect on mfERG amplitudes was detectable after 10 days. In the recordings that were acquired 4 weeks after the laser treatment, an mfERG area with a reduced amplitude corresponded to one of the laser spot areas (Fig. 5A). In all three mice that were treated this way, the 100- μ m laser spots were difficult to discern.

Therefore, in a second scheme, we selected laser spots of 300- μ m size for laser treatment. In Figure 6, recordings are presented in a similar way as in Figure 5. Although laser spots right to the ONH were induced with 30 J/cm², laser spots on the left side were obtained with a retinal irradiance of 10.1 J/cm². In the two recordings presented in Figure 6, the mfERG amplitudes of areas corresponding to laser spots of 30 J/cm² were reduced relative to the surrounding areas. This effect was present 10 days and 4 weeks after laser treatment. In contrast, the laser spots obtained with lower energies (10.1 J/cm²) did not affect the mfERG amplitudes.

We further analyzed the effect of 300- μ m laser spots on the mfERG amplitudes in a group of five mice. Because the laser

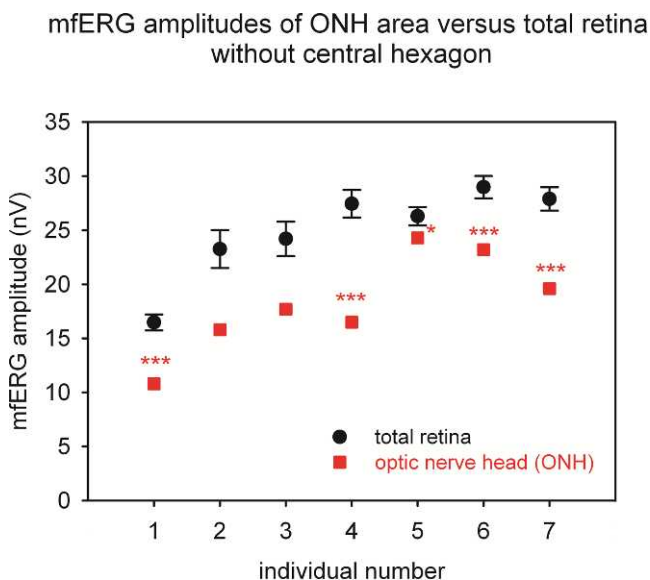


FIGURE 4. The mean of the total retinal mfERG amplitudes without the central amplitude (black dots, ± SEM) compared to the central amplitude corresponding to the ONH area (red quadrates) in an array of 19 hexagons. All values are reported as mean ± SEM. The asterisks indicate a significant difference (* $P = 0.037$; *** $P < 0.001$; one-sample t -test) between total retina and ONH.

spots corresponded to two to three hexagons of the multifocal stimulus, we selected the lowest amplitude of these two to three hexagons for comparison with nontreated, non-ONH areas. In Figure 7, the mfERG amplitudes to each hexagon stimulated with the 30 J/cm² (green, routes) and the 10.1 J/cm² (red, quadrates) laser spots are plotted for each of five individuals. In addition, the response amplitudes of the nontreated, non-ONH areas are displayed for comparison (black, dots). Figure 7A shows the amplitudes from recordings performed 10 days after laser application, whereas Figure 7B displays the data 4 weeks after photocoagulation. At both points in time, the mfERG responses in the areas corresponding to the 30 J/cm² laser spots were significantly lower than those in the nontreated retinal areas. The reduction is more pronounced 4 weeks after treatment compared with 10 days after treatment. A statistically significant effect of laser spots with 10.1 J/cm² energy has been found only for mouse number 5 at 10 days after treatment. Although other laser spots of 10.1 J/cm² failed to reach statistically significant effect (one-sample t -test) on mfERG amplitudes, a trend toward lower mfERG amplitudes could be observed for all individuals at both points in time.

DISCUSSION

The mfERG technique is a useful tool for investigating the spatial distribution of retinal function and for detecting spatially restricted retinopathies. In the current study, we describe the results of mfERG measurements in mice using a modified apparatus originally designed for use in human

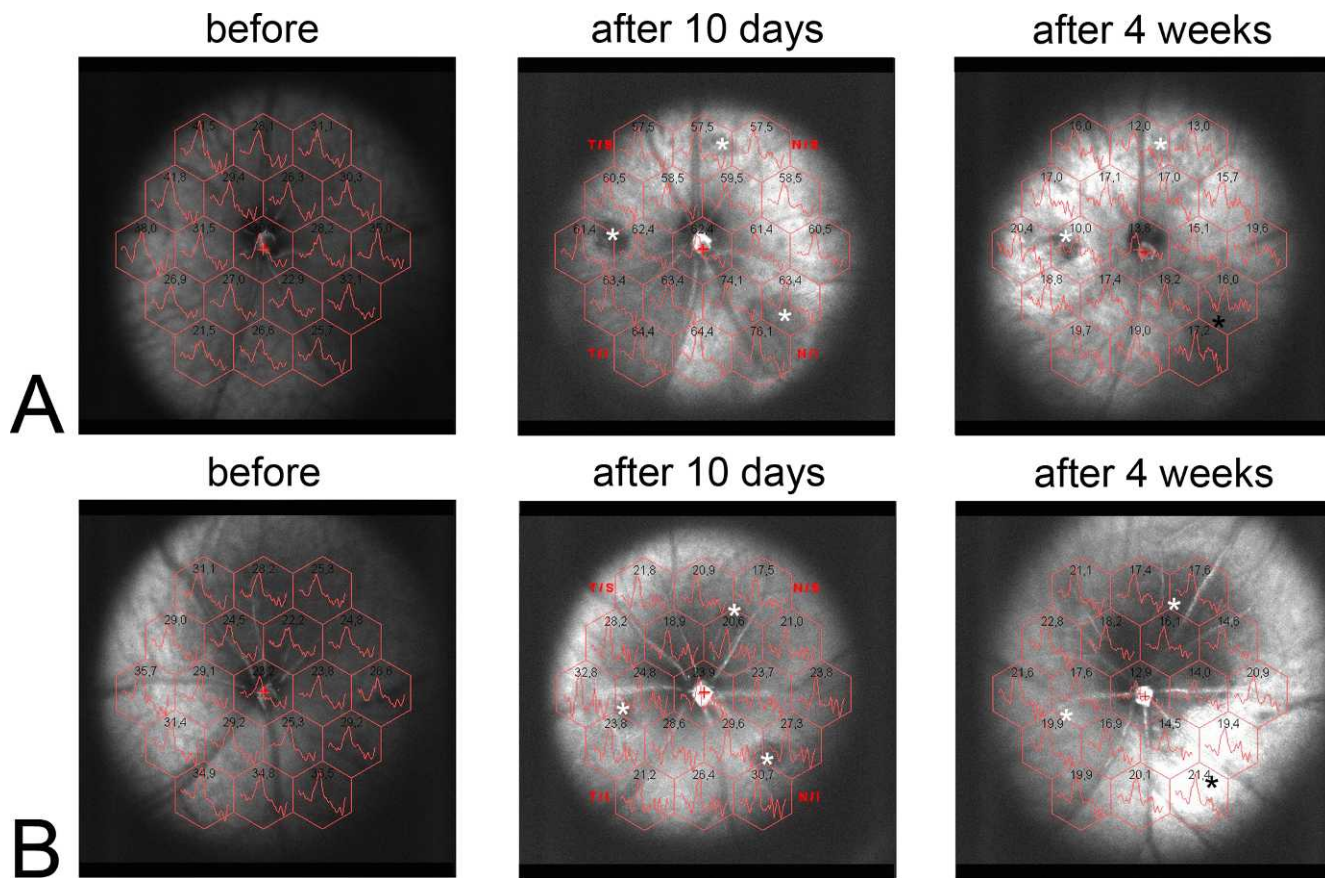


FIGURE 5. SLO images with corresponding mfERG amplitudes in two laser-treated eyes (A, B). SLO-mfERG recordings are presented before, 10 days, and 4 weeks after laser treatment. The three laser spots applied had a 100- μ m diameter and a total energy of 30.6 J/cm². The asterisks represent retinal areas treated by laser photocoagulation.

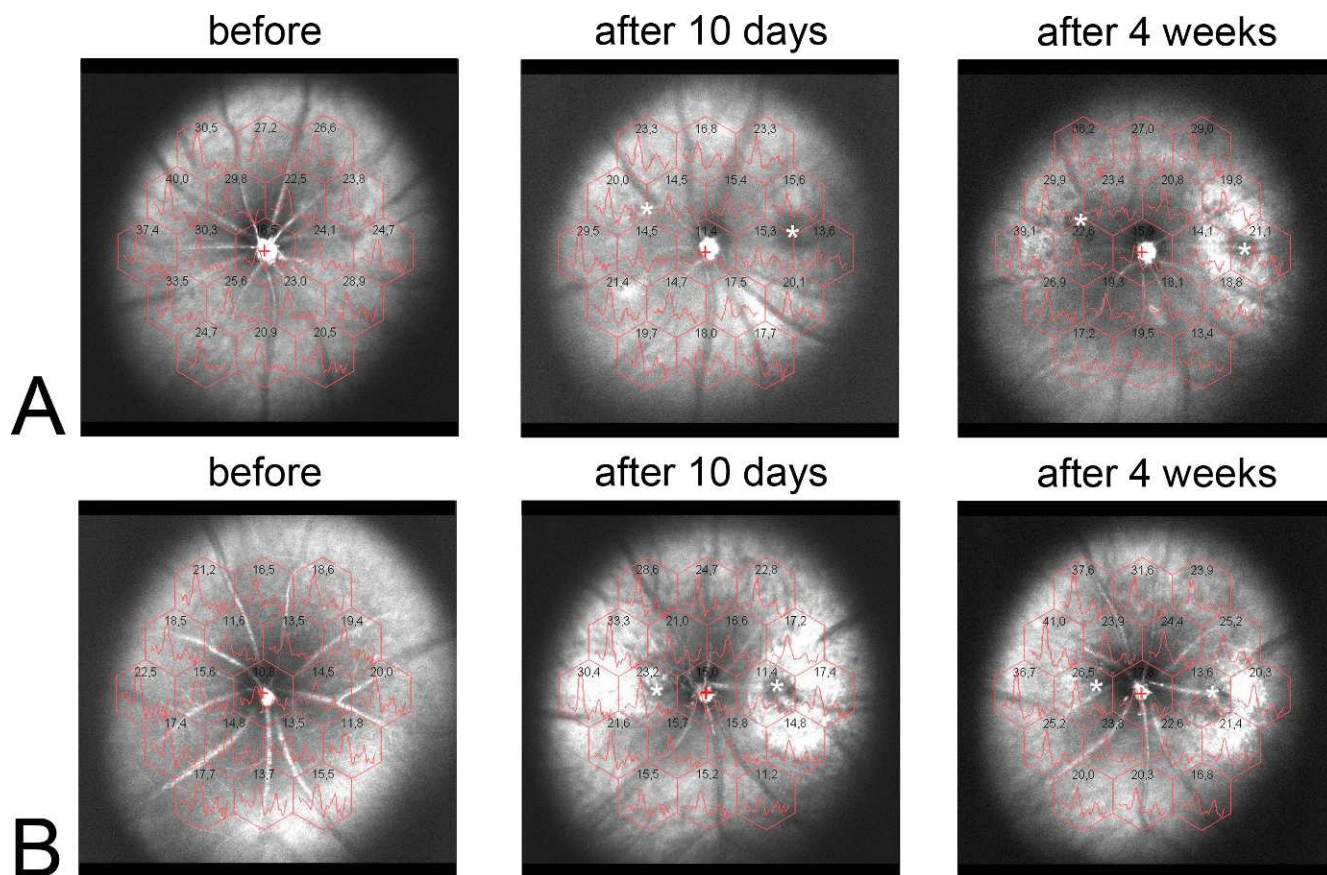


FIGURE 6. SLO images with corresponding mfERG amplitudes in two laser-treated eyes (A, B). SLO-mfERG recordings are presented before, 10 days, and 4 weeks after focal laser treatment. The two laser spots of 300- μm diameter differ in laser energy applied. Spots on the right side of the ONH represent 30 J/cm², spots on the left side 10.1 J/cm². The *asterisks* represent retinal areas treated by laser photocoagulation.

subjects. With the same equipment, a retinal image was obtained. We found that first-order kernels of mfERGs were readily recordable. In a first set of experiments, we tested various stimulus conditions to find the optimal condition for mfERG recording. In mice, the ERGs are strongly driven by rod signals,⁷ resulting in slow signals that may adapt when the interstimulus time interval is too short. Therefore, it can be expected that a slow presentation rate of multifocal ERG stimuli will result in larger mfERG amplitudes. This was indeed the case. These findings are in agreement with the mfERG data in the rat.⁵ However, as a disadvantage, more dark steps result in longer recording times, in which small movements may play a significant role. We conclude that measurements with four dark steps between the stimuli resulted in optimal recordings with sufficient large ERGs in a time range that is short enough to avoid movement artifacts.

A further important purpose of our study was to establish a correlation between mfERG data and the presence of visible retinal areas that are expected to display functional differences with the surrounding areas (the ONH; areas with photocoagulations). In contrast to humans and nonhuman primates, mice lack a macular region. In contrast to previous studies,^{8,9} we obtained mfERG responses from areas that could be identified on a retinal image using the SLO. By centering some hexagons of the multifocal stimulus on the ONH and on photocoagulations, we were able to establish a correlation between morphological and functional characteristics. The data clearly showed that the retinal image and the projected stimuli were adequately aligned. However, some problems remain. It cannot be excluded that small misalignments between the retinal

image and the multifocal stimulus caused by interindividual differences in optical quality of the eye media remain. In addition, stray light still plays a role, as the data with the added surround luminance show.

To test mfERG technique, we searched for a spatially restricted retinal area with reduced excitability compared with surrounding retinal areas. Anatomically, the ONH is an area with no photoreceptors. Thereby, a stimulus covering the ONH should elicit no response. Although the response was indeed smaller, it was not completely extinguished. Interestingly, in humans or larger animals like pigs, hexagons corresponding to the ONH also elicited a response.^{2,9} Shimada and Horiguchi¹⁰ pointed out that this remaining activity could be caused by stray light artifacts and by reflection from myelinated nerve fibres of the ONH and neighboring hexagons. In animal models with smaller body size, like mice and rats, ONH-related potentials were even indistinguishable from the remaining retinal amplitudes.^{3,5} Given the small size of the rodent retina, stray light artifacts are possibly more pronounced than in larger animal models. This could also be the cause for the measured responses in the mice reported in the present study. Reflections at the ONH and possibly at the coagulated areas, where the RPE may be absent, may be an additional cause for stimulation of areas outside those covered by the hexagons. Finally, the hexagons often also covered parts of the retina that contain photoreceptors and postreceptoral neurons. However, the responses to the stimuli covering the ONH and the coagulated areas are substantially lower, proving that damaged areas can be detected with mfERG. In addition,

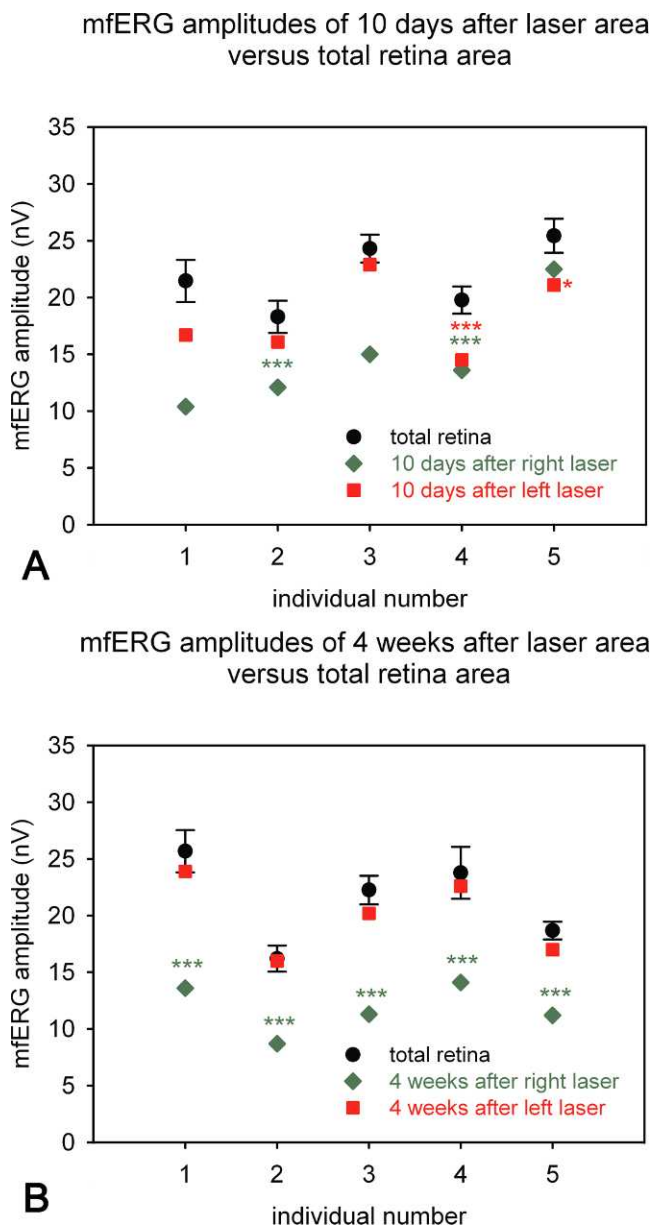


FIGURE 7. mfERG amplitudes in areas of laser treatment compared with amplitudes in areas not affected by laser treatment in five individuals. Amplitudes in areas corresponding to laser spots of 30 J/cm^2 (green routes) and amplitudes in areas corresponding to laser spots of 10.1 J/cm^2 (red quadrates) are compared with amplitudes of nontreated ONH retinal areas (black dots). (A) Amplitudes from recordings performed 10 days after laser application. (B) Amplitudes 4 weeks after photocoagulation. All values are reported as mean \pm SEM. The asterisks indicate a significant difference ($^*P = 0.029$; $^{***}P < 0.001$; one-sample *t*-test).

the data strongly suggest that the mfERG stimulus and the SLO retinal images are well aligned.

The issue that stray light plays a role in the measured mfERG responses is also shown by the fact that illuminating the areas outside the mfERG array results in a response reduction. This is in agreement with previous findings in rodents⁵ as well as in humans.¹¹

Interestingly, the ERG responses at laser lesions are not fully extinguished. Although stray light cannot be excluded as a source for residual responses at the lesion areas, the fact that these responses are diminished indicates that they originate

substantially in the areas themselves. Apart from stray-light effects, other mechanisms may dominantly account for the residual ERG responses. Histological analyses of retina sections at the lesion areas show residual vital photoreceptors with outer segments (Supplementary Fig. S1). The activity of these photoreceptors and the connected postreceptor neurons likely generate an ERG response at the lesion areas. Photoreceptors survive laser photocoagulation because the applied energy is primarily absorbed by the pigment epithelium. That can be seen also by the fact that the main lesion is under the RPE. Only as a secondary consequence, it affects the surrounding photoreceptors by heat transmission. It is also possible that photoreceptor cells from untreated surrounding areas migrate to the damaged area leading to a decreased lesion size over time.¹² The hexagon covering the ONH also covers parts of the photoreceptor containing surrounding retina that contributes to the ERG response.

Laser-Induced Focal Retinopathy

The idea of inducing focal retinopathies by laser photocoagulation to validate the mfERG technique is not new. In a pig model, Kyhn et al.¹³ tested the spatial resolution of the mfERG detecting laser spots down to a size of 1.2 mm. With our setting, we detected laser spots with 300- μm diameter. Laser spots of 100 μm were visible in SLO images but were rarely detected in the mfERG recordings. Apparently, a minimal spot size has to be used to be detectable in the mfERG. Our data suggest that the spatial resolution of the mfERG recording is between 100 and 300 μm . In addition, there was a clear influence of the energy applied on the measured mfERG amplitudes. Using 300- μm laser spots of 10 J/cm^2 of energy, no response reductions were measured. This is possibly due to the smaller damage in the retina leaving a substantial part functional.

CONCLUSION

In this study, we present a novel technique for recording mfERGs with simultaneous retinal image recording for retina research. In contrast to earlier reports on rodents, we could detect the ONH area in the mfERG recordings. We could demonstrate good alignment between SLO images and mfERGs in a laser model of focal retinopathy. This study gives evidence that a reproducible mfERG technique is able to reliably detect the functional consequences of local treatment, for example, local damage as in the present article, or the effects of local interventions, for instance through injections of viruses.

Acknowledgments

The authors thank Benjamin Dammann, Manfred Stasche, and Joachim Finger from Roland Consult for technical support.

Parts of this work were presented at the 50th International Society for Clinical Electrophysiology of Vision Symposium Valencia, Spain, June 4–8, 2012.

Supported by Deutsche Forschungsgemeinschaft (DFG) Jo 324/6-2 (Emmy Noether Program [AMJ]) and DFG Jo 324/10-1 (AMJ).

Disclosure: **R.M. Dutescu**, None; **S. Skosyrski**, None; **N. Kociok**, None; **I. Semkova**, None; **S. Mergler**, None; **J. Atorf**, None; **A.M. Jousen**, None; **O. Strauß**, None; **J. Kremers**, None

References

- Birch DG, Anderson JL. Standardized full-field electroretinography. Normal values and their variation with age. *Arch Ophthalmol*. 1992;110:1571–1576.

2. Sutter EE, Tran D. The field topography of ERG components in man—I. The photopic luminance response. *Vision Res.* 1992; 32:433–446.
3. Ball SL, Petry HM. Noninvasive assessment of retinal function in rats using multifocal electroretinography. *Invest Ophthalmol Vis Sci.* 2000;41:610–617.
4. Moren H, Gesslein B, Andreasson S, Malmstro M. Multifocal electroretinogram for functional evaluation of retinal injury following ischemia-reperfusion in pigs. *Graefes Arch Clin Exp Ophthalmol.* 2010;248:627–634.
5. Nusinowitz S, Ridder WH III, Heckenlively JR. Rod multifocal electroretinograms in mice. *Invest Ophthalmol Vis Sci.* 1999; 40:2848–2858.
6. Gyorloff KW, Andreasson S, Ghosh F. mfERG in normal and lesioned rabbit retina. *Graefes Arch Clin Exp Ophthalmol.* 2006;244:83–89.
7. Jeon CJ, Strettoi E, Masland RH. The major cell populations of the mouse retina. *J Neurosci.* 1998;18:8936–8946.
8. Moren H, Undren P, Gesslein B, Olivecrona GK, Andreasson S, Malmstro M. The porcine retinal vasculature accessed using an endovascular approach: a new experimental model for retinal ischemia. *Invest Ophthalmol Vis Sci.* 2009;50:5504–5510.
9. Kyhn MV, Kiilgaard JF, Lopez AG, Scherfig E, Prause JU, la Cour M. Functional implications of short-term retinal detachment in porcine eyes: study by multifocal electroretinography. *Acta Ophthalmol.* 2008;86:18–25.
10. Shimada Y, Horiguchi M. Stray light-induced multifocal electroretinograms. *Invest Ophthalmol Vis Sci.* 2003;44: 1245–1251.
11. Hood DC, Wladis EJ, Shady S, Holopigian K, Li J, Seiple W. Multifocal rod electroretinograms. *Invest Ophthalmol Vis Sci.* 1998;39:1152–1162.
12. Busch EM, Gorgels TG, van Norren D. Filling-in after focal loss of photoreceptors in rat retina. *Exp Eye Res.* 1999;68:485–492.
13. Kyhn MV, Kiilgaard JF, Scherfig E, Prause JU, la Cour M. The spatial resolution of the porcine multifocal electroretinogram for detection of laser-induced retinal lesions. *Acta Ophthalmol.* 2008;86:786–793.